Molecular architecture for DNA wiring

Judit Pérez, Samuel Dulay, Mònica Mir, Josep Samitier

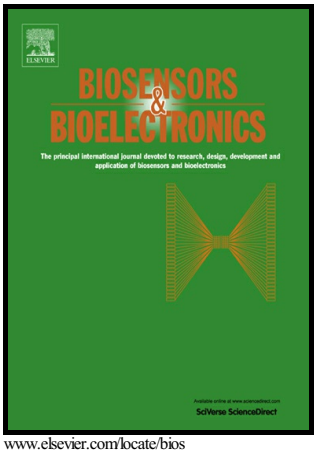

www.elsevier.com/locate/bios

PII: S0956-5663(18)30650-X
DOI: https://doi.org/10.1016/j.bios.2018.08.050
Reference: BIOS10714

To appear in: *Biosensors and Bioelectronic*

Received date: 12 June 2018
Revised date: 14 August 2018
Accepted date: 21 August 2018

Cite this article as: Judit Pérez, Samuel Dulay, Mònica Mir and Josep Samitier, Molecular architecture for DNA wiring, *Biosensors and Bioelectronic,* https://doi.org/10.1016/j.bios.2018.08.050

Molecular architecture for DNA wiring

Judit Pérez[a1], Samuel Dulay[a1], Mònica Mir[*a,b,c], Josep Samitier[a,b,c]

[a]Nanobioengineering group, Institute for Bioengineering of Catalonia (IBEC) Barcelona Institute of Science and Technology (BIST), 12 Baldiri Reixac 15-21, Barcelona 08028, Spain

[b]Centro de Investigación Biomédica en Red en Bioingeniería, Biomateriales y Nanomedicina (CIBER-BBN), Monforte de Lemos 3-5. Pabellón 11, 28029 Madrid, Spain

[c]Department of Electronics and Biomedical engineering, University of Barcelona, Martí i Franquès 1, 08028 Barcelona, Spain

[*]Corresponding author: mmir@ibecbarcelona.eu

Abstract

Detection of the hybridisation events is of great importance in many different biotechnology applications such as diagnosis, computing, molecular bioelectronics, and among others. However, one important drawback is the low current of some redox reporters that limits their application. This paper demonstrates the powerful features of molecular wires, in particular the case of S-[4-[2-[4-(2-Phenylethynyl)phenyl]ethynyl]phenyl] thiol molecule and the key role that play the nanometric design of the capture probe linkers to achieve an efficient couple of the DNA complementary ferrocene label with the molecular wire for an effective electron transfer in co-immobilised self-assembled monolayers (SAMs) for DNA hybridisation detection. In this article, the length of the linker capture probe was studied for electron transfer enhancement from the ferrocene-motifs of immobilised molecules towards the electrode surface to obtain higher kinetics in the presence of thiolated molecular wires. The use of the right couple of capture probe linker and molecular wire has found to be beneficial as it helps to amplify eightfold the signal obtained.

Keywords: DNA hybridisation, bioelectronics, electron transfer rate constant, molecular wires, electrochemistry, ferrocene, biosensor.

1. INTRODUCTION

The simple structure of two couples of nucleotides; A-T and C-G in the DNA double helix arrangement, which write our complex genetic information, has been used for disparate functionalities in different biotechnology areas. The best-known application is in the biomedical field, where DNA hybridisation can diagnose many different diseases, it can tell our genetic predisposition to many illnesses or determine the paternity with a lock of hair. Other area less widespread, where the unique electronic, molecular recognition and self-assembly advantages of DNA structure has been exploited, is the field of molecular electronics. In the area of bio-microelectromechanical systems, DNA has been used as a promising molecular switch, letting the current to pass through the DNA duplex in a nanogap device (Zaffino 2014). Also the DNA-based electrical circuits has been proposed by Dr. Porath, claiming the ability of DNA for conducting electrical charge over considerable distance (Livshits 2014). Moreover, in the computing area, the Weizmann Institute of Science fabricated the first programmable computer silicon microchips-free, which was composed of enzymes and DNA molecules (Lovgren 2003) and eleven years after it was possible to store a JPEG picture, an audio or a movie in a DNA digital data storage (Ezziane 2005; Dong 2015; Shipman 2017).

In most cases, it is required the immobilisation of a capture sequence of DNA onto the transducer surface and the detection of the hybridisation event with the complementary strand. The hybridisation can be detected through direct transduction, inducing changes in electrochemical parameters such as conductivity or capacitance (Paleček 1988; Porath 2000), but at low sensitivity due to the high background signal. This drawback is overcome with redox indicator attached to the duplex. The redox enzyme labels are the ones most used in electrochemical detection since they provide higher signal amplification. Nevertheless, it requires the use of additional reagents and steps in the

[1] The two first authors have contributed equally.

bioelectrochemical measurement, increasing the complexity, time and cost of the sensing and its integration in the final device. Moreover, enzymes are unstable under certain temperature and cannot be directly used in PCR primers and their use requires the addition of an intermediate linker increasing again the reagents and the steps.

Ferrocene based molecules does not have these inconveniences, while having a well-established chemistry, which make these molecules an attractive reagent-less redox reporters. These molecules are neutral compounds stable in the presence of water and air, which makes them very interesting for biological applications. They are highly reversible redox systems and can be switched between ferrocene and ferrocenium cation at low potentials (Seiwert 2008). However, it has been reported that this type of label gives low current detection due to its lone electron obtained from each ferrocene, which must be transferred to the electrode in the most efficient way to allow detection. Some efforts where focused in this direction, and conductive redox molecules where included in the design of these platforms to help the transfer of the electrons produced in the label to the transducer. The intercalation of redox molecules positively charged with an appropriate size for being entrapped inside the DNA loop, such as $Ru(NH_3)_6^{3+}$, Zn^{+2}, Co^{+2}, and Ni^{+2}, where used to enhance the ferrocene labelling (Xu 2004; Cheng 2015). Another strategy for electron transfer enhancement is the use of the called molecular wires (MW); organic molecules that string together double bonds from aromatic rings, ethylene groups and/or acetylene groups with π-π coupling for building blocks of conductive molecules attached by self-assembling on the transducer surface. The MW, as the redox intercalators, assists in the electron transfer but that one in a reagent-less manner. This type of molecules was widely studied in molecular electronics, like oligo(phenylene ethynylenes) (OPEs), and oligo(phenylenevinylenes) (OPVs) (Swager 1998; Flatt 2003; Ulgut 2008; Eckermann 2010). The main application of MWs with biomolecules was focused in the wiring of protein redox heme to the electrode surface (Hess 2003; Trammell 2007) but its combination with DNA has been rather scarce. Umek et al. reported one example with DNA biosensing, where a mixed monolayer of thiolated capture probe and molecular wire facilitated the hybridisation detection, but for this aim was required a second hybridisation with a labelling DNA containing eight ferrocene-modified nucleotides, which hold in close proximity to the molecular wire (Umek 2001). This DNA sandwich configuration require extra reagents and turn the system into a complex platform. Therefore, a principal challenge in DNA bioelectronics is to improve electron transfer properties to obtain an optimal hybridisation detection in a straightforward and reagent-less manner for the development of the technology of interest.

This paper aims to study an efficient and reagent-less strategy for transferring electrons from ferrocene labels in complementary DNA to the electrode sensor. For this purpose, a combination of a mixed SAM containing a MW and an appropriate design of the capture probe linkers to bring closer the ferrocene to the wiring molecules was performed. Here, the selected molecular wire used is readily available commercially suppressing any needs for synthesis in the lab, making it easily adaptable. Moreover, the size and structure of the molecular wire provides the preferred platform for SAM's formation and stability, since it is not promoting steric hindrance. The electrode surface was modified by mixed SAM with thiolated DNA capture probe, 6-mercaptohexanol (MCH) as a blocking agent and S-[4-[2-[4-(2-Phenylethynyl)phenyl]ethynyl]phenyl] thiol, acting as molecular wire. The ferrocene moiety comes into play from the hybridisation of the ferrocene-labelled complementary DNA strands with the co-immobilised DNA probe sequences on the working electrode (Figure 1a). To test the performance of the MW, the surface of an electrochemical sensor with a mixed monolayer of ferrocene thiolated molecule (Thiol-Fc) and the MW was studied to confirm the role of the latter as enhancing agent of the electron transfer rate constant between the reporters and the working electrode. Two DNA sensor architectures, which left the ferrocene label at different positions respect the MW and the electrode surface, were studied. For this purpose, two length of capture probe linkers (C3 and C12) were used for this purpose. Upon hybridisation, the reported signal was studied in both platforms.

2. EXPERIMENTAL SECTION

2.1. Materials

6-(Ferrocenyl)hexanethiol (Thiol-Fc*), S-[4-[2-[4-(2Phenylethynyl)phenyl]ethynyl]phenyl]thiol* (MW) and *6-Mercaptohexanol* (MCH*)* were purchased from Sigma Aldrich as well as K_2HPO_4, KH_2PO_4, EDTA and 1% Tween. NaCl was bought from Panreac and Tris-HCl, from Fluka. Modified oligonucleotides were purchased from Biomers (Ulm, Germany); The capture probe (5'-CGG AGG TAC ATT CGA CTT GA-3') having two different thiol alkyl linkers were used; 3'-mercaptopropane oligonucleotide (thiol-C3-DNA) and 1-mercapto-6-hexadione-7-hexamine oligonucleotide (thiol-C12-DNA). A complementary sequence (5'-TCA AGT CGA ATG TAC CTC CG) was ordered

as target probe functionalised with a ferrocene label at 5'with C5 linker (DNA-Fc). Screen printed electrodes (1 mm diameter circular Au films) were purchased from DropSense,S.L. (Llanera, Spain). Photolithographed arrays (Au electrodes of 1mm diameter for each of the 64 gold working electrodes and gold conducting paths) of gold electrodes were prepared at IBEC clean room facilities (Barcelona, Spain). The surface plasmon resonance spectroscopy substrates (18x18 mm^2, 50nm Au, 2nm Ti, 0.7mm D263 Glass) were provided by NTB Interstaatliche Hochschule für Technik Buchs (Germany).

2.2. Methods

2.2.1. Molecular wire deprotection

The molecular wire was prepared from the thioacetate form *S*-[4-[2-[4-(2-Phenyl ethynyl)phenyl]ethynyl]phenyl] thioacetate by decapping the thiol to allow its surface immobilisation on gold. The thioacetate was dissolved in ethanol under inert atmosphere and NaOH solution was added in a drop-wise fashion. The reaction was left to reflux for 2 hours and cooled at room temperature (RT). The mixture was neutralised with 2 M HCl and transferred to a different funnel. To separate the organic layer, degassed diethyl ether and degassed water were added. The organic layer was then washed with degassed water and dried over Na_2SO_4 before removing the solvents at 40ºC using a rotary evaporator. The molecular wire was then recovered from the evaporator wall adding 60 ml of ethanol. 1 mM aliquots were prepared and stored at -20ºC.

2.2.2. Electrode array pre-treatment

The cleaning procedure differed depending on the electrodes since some cleaning methods were found to damage the serigraphic ones. Screen printed electrodes were cleaned electrochemically with H_2SO_4 (0.5 M) programming 15 cyclic voltammetry scans from 0.2 to 1 V at 0.5 Vs^{-1}. Photolithographed Au chip arrays from IBEC were previously cleaned by rinsing them with cold piranha solution (H_2SO_4 : H_2O_2, 5 : 1 v/v ratio). After cleaning, the electrodes were washed with MilliQ water and dried with N_2 gas. The cleaning procedure was always done prior to electrode bio-functionalisation. For the SPR Au chip, it was cleaned with soap and deionised water then subsequently sonicated in ethanol for 5 minutes and thereafter it was exposed to UV light for 10 minutes before mounting them into the SPR electrochemical cell.

2.2.3. Mixed monolayer preparation

The mixed monolayer solution prepared with $NaHPO_4$ (1 M) in 137 mM NaCl, 2.7 mM KCl and 10 mM phosphate buffer solution, pH 7.4 (PBS) were then incubated on gold electrode surface for 8–12h at RT inside the humidity chamber protected from light to form co-immobilised SAM. The immobilised SAMs used were the following: a) Thiol-Fc, b) Thiol-Fc with the MW, c) Thiol-C_3-DNA capture probe with MCH, and d) Thiol-C_3-DNA capture probe with MCH and MW, e) Thiol-C_{12}-DNA capture probe with MCH, and f) Thiol-C_{12}-DNA capture probe with MCH and MW. After the first immobilisation, electrodes were rinsed with 10 mM NaCl, 5 mM Tris-HCl and 1% Tween and dried gently with N_2Thiol-Fc. Subsequent backfilling (1 hour) using MCH has been done to cover the possible monolayer defects and for avoiding non-specific adsorption. Hybridisation was carried out with complementary DNA-Fc at RT inside the humidity chamber protected from light for one hour of incubation wherein the complementary target sequence was prepared in a hybridisation buffer composing of 1 M NaCl, 10 mM TrisHCl, and 1 mM EDTA.

2.2.4. Electrochemical measurements

Cyclic voltammetry (CV) measurements were performed with a Versastat3 (AlphaOmega Electronics, Madrid) in a three-electrode system with Au electrodes as working electrodes, Pt as counter electrode and a Ag/AgCl as a reference electrode. All voltammograms were obtained at RT under ambient conditions and measurements were carried out in a 0.1 M NaCl solution.

2.2.5. Surface plasmon resonance (SPR) measurements

SPR experiments were performed in a RES-TEC instrument (Resonant Technologies GmbH, Framersheim, Germany). Kinetic and static measurements were performed on SPR chips as follows; A baseline scan of PBS was measured until stabilisation of the signal at a constant flow rate of 300 µl/min. Then, 100 µM Thiol-Fc solution was injected in the SPR cell for 2 hours to immobilise a monolayer of this molecule and subsequently PBS was introduced to the system

as a rinsing step to reach the initial refractive index in the interface to calculate the increase of signal due to Thiol-Fc immobilisation. At this point the kinetics was paused and a scan at different angles was performed. After the measurement at different angles, kinetic measurement was continued and 900 µM solution of the molecular wire was recirculated inside the SPR cell for 1 hour. A last scan was performed after the molecular wire solution was substituted with PBS to perform once again a static measurement. All scans were taken from 44 to 70 degrees with the flow stopped. In wired DNA detection, a mixed monolayer of DNA:MW (10 µM:10 µM) was left to flow for one hour. To help the DNA immobilisation and diminish electrostatic repulsion, NaH_2PO_4 (1 M) solution was used as the dilution buffer. Afterwards, hybridisation of 3.3 µM DNA-Fc prepared in PBS was done. Adsorption events of these macromolecules onto the chip surface cause a shift in the resonance angle, which were tracked in both dynamic (kinetic) and static (angle scan) measurements analysed and fitted with Winspall Software from Max Planck Institute (Germany). Baseline measurements were considered in PBS.

3. RESULTS AND DISCUSSION

3.1. Electron transfer of Thiol-Fc through the MW

To test the performance of the selected MW to improve the electron transfer of ferrocene labels, a mixed monolayer of a thiolated ferrocene molecule with the MW was prepared as a model system. Its redox signal was detected electrochemically, and the monolayer was characterised with SPR. The expected mixed monolayer including both the MW and the redox active molecules is represented in Figure 1b.

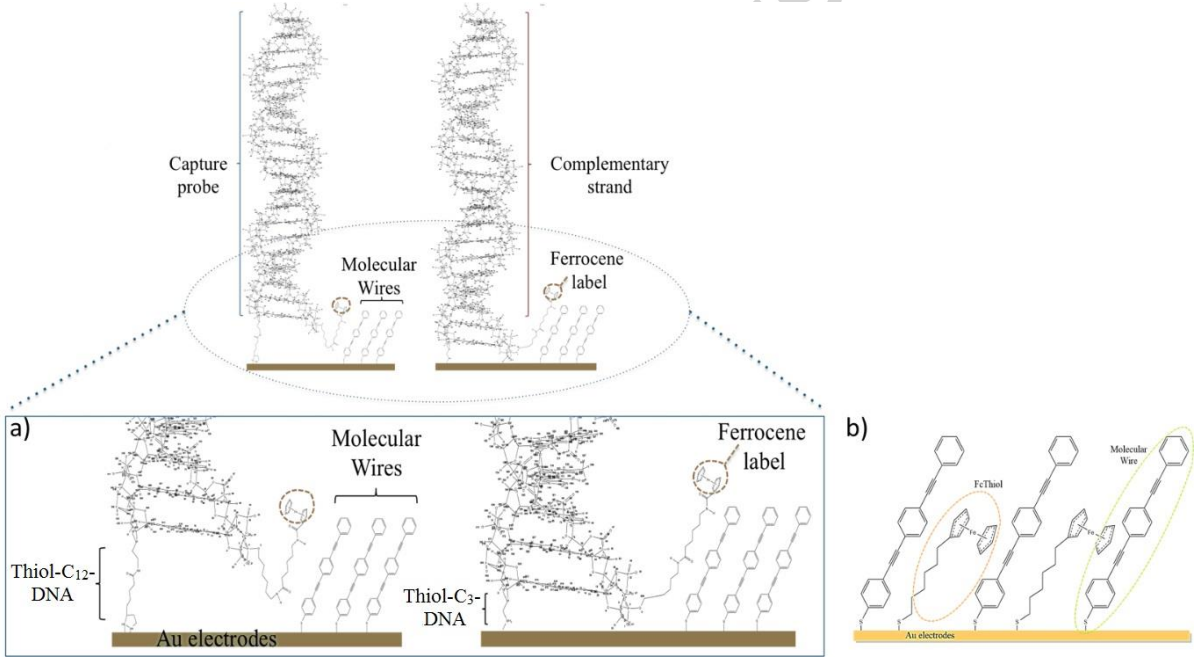

Fig. 1. Schematic representation of the mixed monolayer of a) MW and hybridised DNA molecules on top of gold electrodes immobilised using two different linkers of thiol-C_3 and thiol-C_{12}. Complementary strands have been redox-labelled with ferrocene molecules to allow electrochemical detection and b) Thiol-Fc (encircled with orange dashed line) with MW (green) on top of gold electrodes. Generated with ChembioDraw 14.0.

3.1.1. Electrochemical characterisation

In cyclic voltammetry (CV) measurements of the oxidation and reduction voltages of the electroactive reversible heterogeneous ferrocene, an increase of the positive and negative faradaic current at these voltages is clearly observed. Ideally in the case of ferrocene and other reversible redox molecules, the scans should result in reversible electrochemical responses when both reduced and oxidised forms of the redox motifs are strongly adsorbed on the electrode showing symmetric peaks and a linear relation between the peak current and the scan rate.

Screen printed gold chips were used to perform the first experiments to determine if the MW included in the design of the mixed monolayer had any effects on the electron transfer from the redox active motifs into the surface of the electrode. In order to compare the ferrocene performance with and without wiring, two different mixed monolayers were prepared: a) with the MW in a mixed monolayer of 1:1 c/c Thiol-Fc:MW, and b) without MW, having a mixed monolayer of 1:5 Thiol-Fc:MCH. In the latter, 5 times molecules of MCH were used to mimic the size of wider MW to achieve similar molecules of ferrocene on the electrode surface. CV was used to test the performance of both monolayer. The results obtained were plotted in Figure 2.

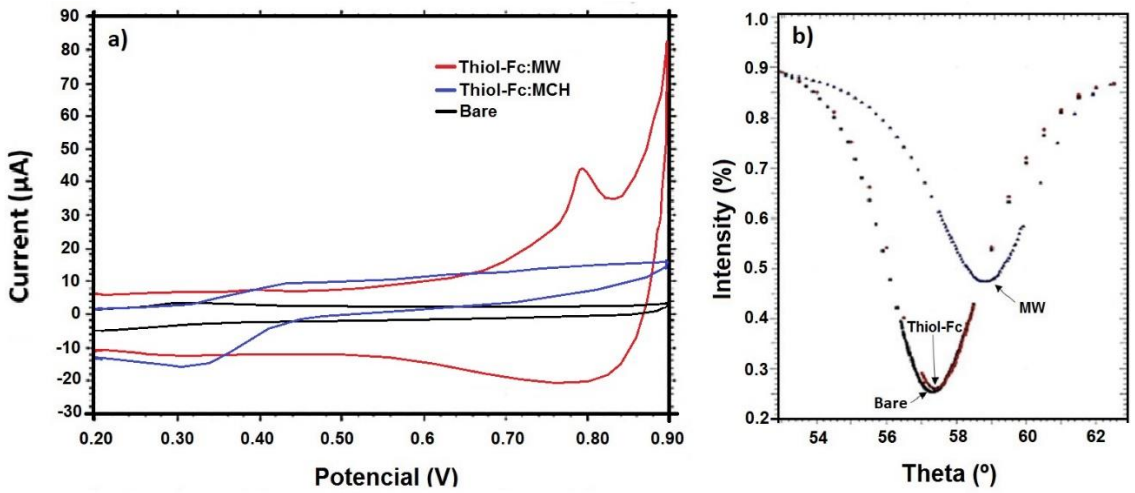

Fig. 2. a) Cyclic voltammetry scans on screen printed electrodes, functionalised with a mixed monolayer of; Thiol-Fc: MW (red) and Thiol-Fc MCH (blue), Bare electrode as negative control (brown dash). CV measurements were carried out in a 0.1 M NaCl solution. b) Angle SPR scans on PBS buffer. Black dots correspond to the scan for PBS baseline in a clean surface of gold chip. Spots in red belong to the Thiol-Fc immobilisation. Scan in blue shows changes associated to the immobilisation of the MW.

The redox peaks described for ferrocene redox reaction are between 0.2 and 0.6 V (Seiwert 2008) and this range may experience a shift depending on the linkers that attached the ferrocene on the surface, and also the transfer mediation of a secondary molecule. This is what is observed in Figure 2a from the CV scan of Thiol-Fc co-immobilised with MCH, where the ferrocene peaks appeared between 0.2 and 0.4 V. Remarkably, in the case of the mixed monolayer of Thiol-Fc with the MW, the ferrocene peak is shifted to values of potential between 0.7 and 0.85 V becoming sharper current peaks and showing 4 times higher current values and shorter distances between oxidation and reduction peaks, due to the faster electron transfer with the MW. These results significantly show that the electrochemical measurements provided a confirmation of the influence of the MW in the shift of the peak and most importantly in the enhancement of the signal detection in redox active self-assembled monolayers.

3.1.2. Electrochemical SPR characterisation

To evaluate the assembly of monolayer formation into gold surfaces, the immobilisation of Thiol-Fc and MW were characterised by SPR. This technique relies on the generation and excitation of surface plasmon polaritrons at the interface between a thin metallic layer at the base of a prism and the dielectric, where the biosensor is placed. From different light incident angles, scans of the surface can be performed and obtain the angle at which there is a minimum of reflected light, where total internal reflection is occurring. When different interaction events occur between molecules on the surface of the SPR sensor changes in the dielectric arise, and so in the resonance frequency, that is detected as a shift in the refractive angle. Surface coverage values can be calculated with this technique providing information about monolayer formation, adsorption/desorption kinetics and interaction events if happening (Boozer 2006).

When immobilisation of the molecules occurred, a shift on the angle of minimum reflection was observed when compared to the initial state. An observed remarkable change on the angle denotes a successful immobilisation of the molecular wires. Both events were reflected on Figure 2b, where angle scans were represented.
The surface coverage in each event of immobilisation or hybridisation was calculated based on the results obtained in SPR experiments (Azzaroni 2008). The mass uptake onto the surface of the electrode was calculated using the experimentally determined relationship shown in Eq (1) obtained by experimental results done in Max Planck Institute (Yu 2004).

$$\text{Eq. (1)} \quad T = \frac{\Delta\theta}{0.19}$$

Figure 2b shows the minimum reflection angles obtained after each immobilisation, being: 57.32º for PBS, 57.40º and 58.83º after Thiol-Fc and MW immobilisations respectively. From eq. (1) the calculated surface coverage ($\Delta\theta$) for the Thiol-Fc immobilisation was 0.42 ng/mm^2 and final value for the mixed monolayer was 7.53 ng/mm^2**.** Considering the 3-D structure of the studied molecules, the theoretical coverage of each of them can be calculated. When we consider a Thiol-Fc molecular diameter of 0.66 nm, a rough estimation of the theoretical coverage for a monolayer of this molecule is 1.47 ng/mm^2. Applying the same principle for the molecular wire having a diameter of 0.46 nm, a value of 3.52 ng/mm^2 has obtained. Although the theoretical values of the obtained surface coverage were only rough estimation, it gave us an image of what can be expected in experimental results, obtaining similar relations of the surface coverage.
The SPR scans shown in Figure 2b were fitted considering the theoretical molecular lengths and refractive indexes of each deposited molecule presented on the table 1 in supplementary material. From the fitting of the SPR scans, relevant information can be subtracted such as the thickness of each immobilised layer. This fitting was carried with Winspall Software from Max Planck Institute (Germany). A thickness of 0.91 nm was obtained for the Thiol-Fc layer that coincide with the theoretical length of this molecules, which indicates that a well organised monolayer was obtained after its incubation. Furthermore, a thickness of 3.18 nm for the immobilisation of the MW was also obtained. Considering the length of 1.18 nm expected from a MW monolayer that led to the formation of a bilayer or a monolayer with adsorbed molecules onto the immobilised ones. Several kinds of possible defects can be created in the monolayer formation such as pinholes, islands and aggregated domains and their occurrence favoured more when metallic surfaces are not perfectly flat (Love 2005). Monolayer packing can be also affected by the tilt angle of the molecules particularly alkane thiols that exhibit a tilt angle of approximately 30º with respect to the normal surfaces (Eckermann 2010). A SAM starts with some molecules lying flat in the surface that will align according to the molecular axis as the concentration increases in their surroundings. Nevertheless, some molecules will remain horizontally flat giving rise to monolayer defects that turn into different local environments. Steric repulsion between different types of molecules in mixed monolayers also play an important role and so the ratio between immobilised molecules is not trivial (Eckermann 2010). Taking the fitting of the SAM thickness and the surface coverage into account, further immobilisations was designed with a different relation than the one already studied (100 µM Thiol-Fc: 900 µM MW), since the MW shows more efficient immobilisation even on a surface already partially occupied

3.1.3. Electron transfer evaluation

The surface plasmon resonance chip used in the experiment was set up in an electrochemical cell, which allows electrochemical measurement at the same time while SPR kinetic measurements were running. CV technique was used to measure the rate of electron transfer (k_{ET}) of the ferrocene redox molecule to the electrode, which is an important property to evaluate the MW performance on electrons wiring. E. Laviron proposed a mathematical method to determine the k_{ET} following the next equation (Laviron 1979).

$$\text{Eq. (2)} \quad k_{ET} = \frac{\alpha n F \upsilon_c}{RT} = (1-\alpha)\frac{nF\upsilon_c}{RT}$$

$$\text{Eq. (3)} \quad \upsilon = E_p - E^0$$

Where n is the number of electrons, T is the temperature and R and F are the international gas and Fadaray's constants respectively and ν is the cathodic and anodic scan rate, obtained from the experimental data required in Eq. (3). E_p is the difference between peak potential and E^0 is the formal potential of the complex which comes from the average of

the anodic and cathodic peak potentials, Ep_a and Ep_c respectively. α is the electron transfer coefficient. This parameter is a measure of the symmetry of the energy barrier of the redox reaction. To determine α, the peak potential Ep is plotted *vs* log *v* considering the anodic and cathodic response and from their slope α can be calculated (Laviron 1979; Trammell 2007; Hong 2013).

In determining the k_{ET}, potentials were applied from 0 up to 1 V at different scan rates: 5, 50, 100, 200, 500, 1000 and 2000 mV/s. The currents obtained were plotted at different scan rate, where it can be seen the different tendency between the voltammograms corresponding to the Thiol-Fc monolayer and the mixed monolayer of this molecule with the MW, in which peaks were more defined and narrower even at higher scan rates (Fig. S1, supplementary material). Following Laviron's proposed method, peak-to-peak separation was plotted vs log. of scan rate wherein, we calculated α and k_{ET} (see Fig S2 in supplementary material).

It has been observed significantly the differences in the slopes between both lines that reflects three orders of magnitude increase on the electron transfer rate constant with the molecular wire, showed when compared to the Thiol-Fc alone. These results clearly show the efficient performance of the chosen MW for the improvement of ferrocene electron transfer. Additionally, the clear increase of the area under the peaks was also observed in the CVs (Fig. S2), In the case of the platform containing the MW were observed more defined shapes and higher currents up to 3 times higher signal (0.5 µA *vs* 14 µA in the wired system).

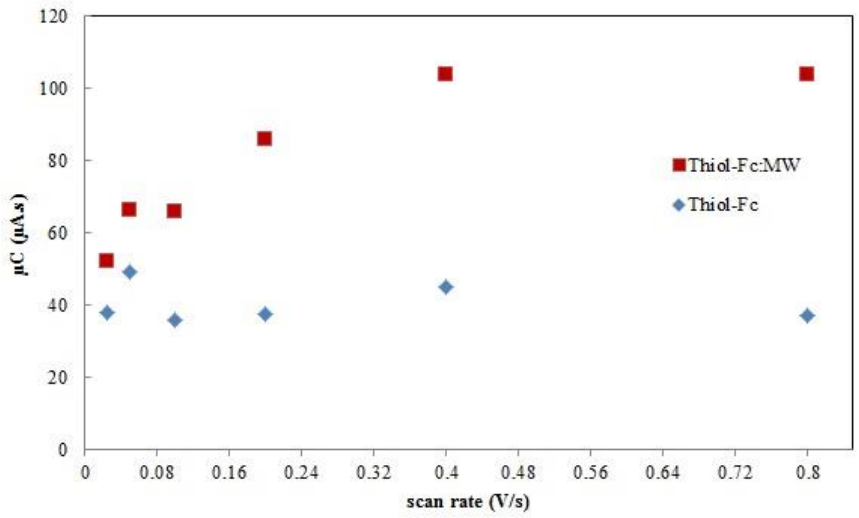

Fig. 3. Charge under the peak curve (Coulomb) at different scan rates for platforms; Thiol-Fc and mixed monolayer of Thiol-Fc with the MW.

3.2. Wired DNA hybridisation detection

The enhancement of the electron transfer rate constant showed in the selected model system; Thiol-Fc and the MW allowed the consideration for further studies. The improvement of electrochemical DNA biosensors with the tested wiring molecules is an interesting application to see the behaviour of the MW in a more complex platform.

Considering the local environment into a SAM; distances between immobilised DNA molecules and their steric repulsion, these affect the electron transfer phenomena from the ferrocene labels to the electrode's surface and cause differences on the possible observed voltammetry scan rates. Eckermann et al. define this as kinetic dispersion or kinetic heterogeneity (Eckermann 2010). To study this effect, two different linkers for the DNA capture probe were considered in the design of the SAMs as illustrated in Figure 1a where the ferrocene moiety in the image shows different distances to the electrode's surface and to the MW; Thiol-C_3-DNA:MW and Thiol-C_{12}-DNA:MW

3.2.1. Immobilisation characterisation

Each layer of the constructed DNA biosensor was monitored and characterised with SPR. Following a similar procedure as previously explained, initial PBS scanning was done to obtain the baseline as shown in Figure 4 (Blue

line). Subsequently, immobilisation of DNA capture probe prepared in NaH_2PO_4 solution was circulated and a PBS scan was performed after (black line) (Fig. 4). A second scan in PBS was performed after the injection of the complementary ferrocene-labelled DNA strand (3.3 µM) as shown in red line. The mixed monolayer was accomplished with the incubation of the MW and after rinsing with PBS (green line) (Fitting parameters for these scans are shown in supporting information).

Result shows the successful immobilisation of the DNA capture probe:MW mixed monolayer, detected as the change on the angle of minimum intensity shifts from 56.19º to 56.85º (Fig. 4). These results obtained can be used to calculate the surface coverage of the immobilised DNA and was found to be 2.15 ng/mm^2. After the hybridisation and mixed monolayer was established, the total surface coverage calculated for the molecules immobilised was 3.53 ng/mm^2. These values were smaller than the ones obtained with the Thiol-Fc since the Thiol-Fc has smaller molecule diameter and so more molecules can be fitted in the same surface. Considering the ss-DNA diameter a theoretical surface coverage (Yu 2004) of 2.22 ng/mm^2 was calculated, which is remarkably closer to the values obtained experimentally, 2.15 ng/mm^2.A thickness value of 1.7 nm was fitted for the immobilisation of the thiolated DNA with the MW and considering the expected length of the DNA of approximately 7.4 nm (Hanwell 2012) (See Fig. S3 supplementary material), this led to the assumption that the surface of the chip was not entirely covered with thiolated DNA SAMs or that part of this capture probe molecules were physically tilted and randomly laying over the gold's surface repulsing other DNA strands to be immobilised rather than forming a homogenously packed DNA layer.

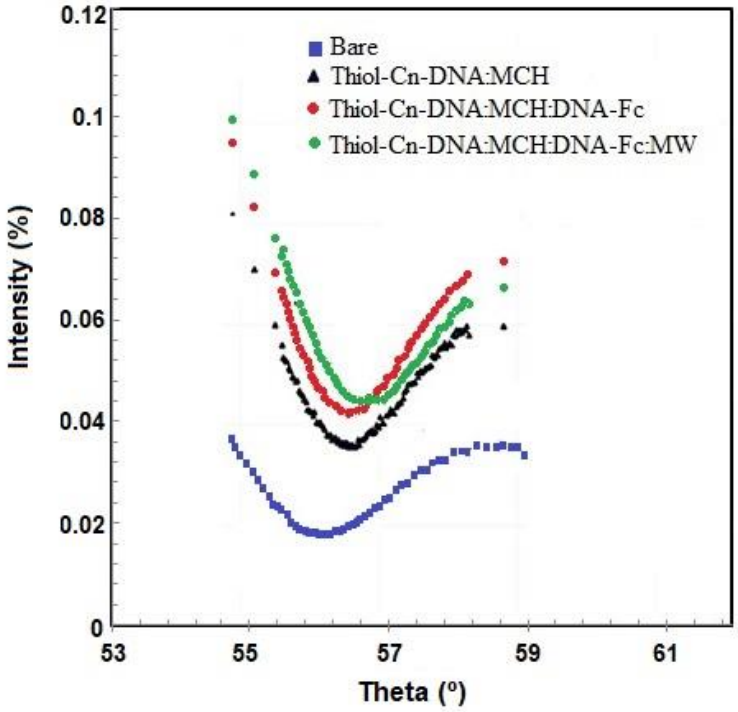

Fig. 4. SPR scans on PBS buffer from 53 to 61 degrees. Blue dots correspond to the scan for PBS in a clean surface gold electrode, becoming the baseline. Line in black belong to the DNA capture probe immobilisation. Scan in red shows changes associated to the hybridisation of the DNA complementary strand with the capture probe. Further immobilisation of MW is detected by the green scan.

3.2.2. Thiol-C_3-DNA:MW wiring characterisation

The chips were functionalised with a mixed monolayer of Thiol-C_3-DNA, MCH and MW (1:4.5:4.5 c/c ratio) and also without the presence of the MW in a mixed monolayer of Thiol-C_3-DNA and MCH (1:9 c/c ratio) as a control. Subsequently, the immobilised DNA probes were left to be hybridised with a complementary DNA ferrocene labelled. Representative results were shown in Figure 5, where the minor ferrocene peaks are hardly seen in the sensor without

MW between 0.2 V to 0.6 V. While in the case of the mixed monolayer containing the MW, the peaks were clearly appeared, with 4 times more current at the same DNA target concentration (0.8 µA vs 0.2 µA in the unwired platform). The redox ferrocene peaks were shifted, appearing between 0.5 and 0.7 V, similar scenario as previously discussed in the direct measured wiring of Thiol-Fc with the MW.

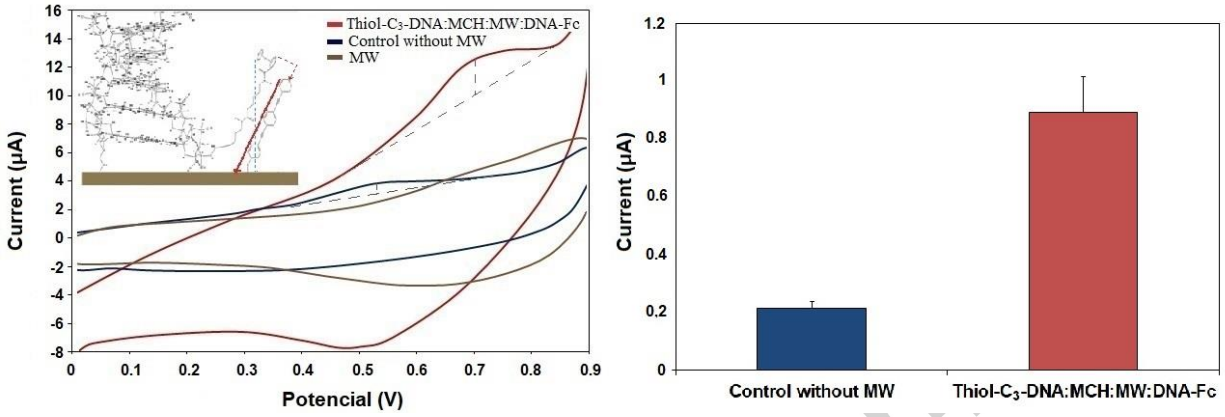

Fig. 5. Cyclic voltammetry scans of: Thiol-C_3-DNA:MCH:MW:DNA-Fc (red) and without wiring effect; Thiol-C_3-DNA:MCH:DNA-Fc (blue). Brown scan corresponds to the signal from a sensor functionalised with a monolayer of MW (1 mM). CV measurements were carried out in a 0.1 M NaCl solution. On the right, summary of results considering current under the peak. (n=3)

These results clearly show, how the MW improved the detection of hybridisation of DNA ferrocene labelled in 5 times. Along with this experiment, a control with the electrochemical response of a MW SAMs alone was carried out to assure that no electroactive species are present into electrode's surface.

3.2.3. Thiol-C_{12}-DNA:MW wiring characterisation

Similar protocol was followed as in previous DNA sensor, where the same type and rates of mixed monolayers were used but, in this case, with a longer linker between the anchoring molecule and the DNA capture probe; Thiol-C_{12}-DNA instead of Thiol-C_3-DNA.

As with previously explained DNA experiments, hybridisation of ferrocene-labelled DNA strands was required and performed with 1 hour of incubation of 3.3 µM DNA-Fc solution. Results from the corresponding electrochemical characterisation with CV were shown in Figure 6. Peaks appeared clearly and sharply between 0.7 and 0.8 V. As happened in the previous reported DNA sensor fabricated with a shorter linker in capture probe, the incorporation of the molecular wire to the mixed monolayer improved the detection of current signal, allowing a much more pronounced electrochemical peak. In this case, the increase of current due to the presence of the MW is 8-fold higher (41 µA) than the direct ferrocene detection (5 µA), which demonstrate the excellence performance and versatility of the studied MW.

Moreover, the design of the interface architecture of the sensor helps in the enhancement of the electron transfer by the MW. Based on the electrochemical signals from both platforms, the thiol-C_{12}-DNA mixed with MW monolayer gave more defined redox peaks similarly appreciated in the obtained peaks in the Thiol-Fc:MW. In thiol-C_{12}-DNA, due to the linker structure, the ferrocene molecules are at the same distance from the electrode surface than the end of the MW. Whereas, the thiol-C_3-DNA capture probe left the ferrocene label of the complementary DNA strand beyond the MW. In this way the electrons produced in the ferrocene label need to cross higher activation energy to be transported by the MW to the electrode surface. This fact results in a higher current observed in the thiol-C_{12}-DNA platform; 41 µA (figure 6), than in the thiol-C_3-DNA based sensor; 0.8 µA (Figure 5). This results further prove that incorporating the MW with an appropriate interface architecture in the surface chemistry of the DNA sensor undoubtedly improved the biosensor performance in terms of signal detection.

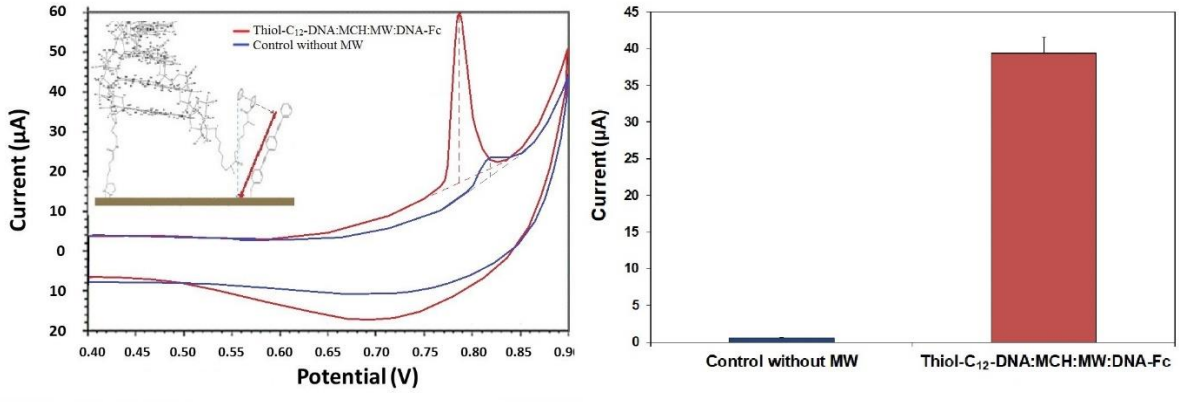

Fig. 6. Cyclic voltammetry scans of Thiol-C_{12}-DNA:MCH:MW:DNA-Fc (Red) and a control without MW; Thiol-C_{12}-DNA:MCH:DNA-Fc (blue). CV measurements were carried out in a 0.1 M NaCl solution. On the right, summary of results considering current under the peak. (n=3)

Several papers on DNA hybridisation detection have showed an improved signal performance through electron transfer mediation. For this purpose, different techniques have been used for increasing the output signal. One of which is the intercalation method where electron transfer mediator like $Ru(NH_3)_6^{3+}$ were embedded into the backbone of the duplex DNA for electron transferring the redox of the label to the electrode surface. With this method, Chem et al. shown an increase in signal by fivefold (Cheng 2015). Another mediation method, where Zn^{+2}, Co^{+2}, and Ni^{+2} were utilised for intercalation within duplex DNA, has shown an improved signal performance around three times (Xu 2004). The charged mediators mentioned above facilitated the electrostatic interaction with the negatively charged DNA duplex and its metallic nature accelerates the transfer of electrons created in the redox label. Another method, closer to our strategy, utilised a mixed monolayer of thiolated capture probe, molecular wire and mercaptoethylene glycol as biosensor interface. Hybridisation transduction required in this case a separate signal probe, attached in a sandwich manner, containing eight ferrocene-modified nucleotides, which hold near the MW. This platform was not tested in the absence of the MW, so there is not report on the signal improvement due to the effect of the MW (Umek 2001).

Table 1 summarises the comparison of the present work with other related works, where the improve of ferrocene electron transfer was studied. In this comparison can be appreciated the higher enhance of signal with our molecular wiring interface. Moreover, in our system, the MW is self-assembled with the capture probe ready to be used without adding extra reagents. The detection technique used is straightforward and cost effective than the rest of reported related literatures, making our wiring interface and excellent configuration for improving electronic signal in DNA platforms.

Table 1. Comparison of the signal performance of the presented work and other electron transfer mediated electrochemical DNA biosensors.

Electrode	***Immobilisation method***	***Electron transfer mediator***	***Detection technique***	***Signal performance improvement***	***Reference***
Au	*SAM*	*oligophenylethynyl*	*DPV*	*Not reported*	*(Umek 2001)*
GCE/ AuNP	*Intercalation*	*$Ru(NH_3)_6^{3+}$*	*SWV*	*5X folds higher*	*(Cheng 2015)*
GCE/PPy	*Intercalation*	*Zn^{+2}, Co^{+2}, and Ni^{+2}*	*EIS*	*3.2X folds higher*	*(Xu 2004)*
Au	*SAM*	*Molecular wire thiol molecule*	*CV*	*8X folds higher*	*This work*

4. Conclusion

In this work, an unexplored electronic DNA interface based on the MW; S-[4-[2-[4-(2Phenyl ethynyl)phenyl]ethynyl]phenyl] thiol, for wiring the electrons produced by a ferrocene label attached to the complementary DNA target was studied. The excellent performance of the studied MW in combination with a careful design of the capture probe linker to bring the ferrocene moiety in close proximity to the MW, results in an excellent sensor interface architecture for DNA hybridisation detection.

A first approach, for testing the MW, was performed with thiolate ferrocene self-assembled with the MW. With this model system, an increase of 4 orders of magnitude of electron transfer constant due to the presence of the MW was observed, showing the excellent possibilities of this MW.

In electronic DNA wiring application, two different capture probe linkers (*Thiol-C_3-DNA* and *Thiol-C_{12}-DNA*) were tested, to study the importance of the designed interfaces to ferrocene positioning with respect MW.

It was appreciated in both platforms that the use of the MW significantly improved the signal detection with more defined redox peaks and higher currents observed in both DNA sensors. Additionally, crucial consequence had the different linker designs in the signal sensor enhancement. Clear differences were observed between both platforms demonstrating the importance of the linker used in the efficiency of electron transfer between the ferrocene and the MW, obtaining eight-fold increase of current with the combination of the MW and the longer linker (that brings ferrocene moiety closer to the MW), while lower increase; four-fold was observed with the shorter linker. The longer linker brings a better configuration for the ferrocene detection on the wire-electrode interface with improved electron kinetics. Comparing with previously reported molecular wiring DNA sensors, our developed platform shows the higher increase of electron transfer, being also, in contrast with previous works, a reagent less, straightforward and cost-effective system.

The molecular wire studied in this paper offers an enormous potential for the improvement of ferrocene signal transfer in DNA hybridisation events. The combination of an efficient linker capture probe design with the MW results in a powerful interface for electronic DNA hybridisation sensing. Next steps require further studies in the applicability of the developed interface in DNA biosensors, such as selectivity, sensitivity, and real sample detection.

Supplementary data

Additional Figures and data can be found in supporting information.

Acknowledgment

CIBER-BBN is an initiative funded by the VI National R&D&i Plan *2008-2011, Iniciativa Ingenio 2010, Consolider Program, CIBER Actions* and financed by the Instituto de Salud Carlos III with assistance from the *European Regional Development Fund*.

The Nanobioengineering group has support from the Commission for Universities and Research of the Department of Innovation, Universities, and Enterprise of the Generalitat de Catalunya (2014 SGR 1442) and is part of the CERCA Programme / Generalitat de Catalunya.

This work was funded by the project MIND from the Spanish Ministry of Economy and Competitiveness TEC2015-70104-P.

M. Funes, and D. Izquierdo (Nanobioengineering group—IBEC) are acknowledged for technical support.

References

Azzaroni, O., Alvarez, M., Mir, M., Yameen, B., and Knoll, W., 2008. The Journal of Physical Chemistry C 112(40): 15850-15859.

Boozer, C., Kim, G., Cong, S., Guan, H., & Londergan, T., 2006. Current opinion in biotechnology 17(4): 400-405.

Cheng, F. F., He, T. T., Miao, H. T., Shi, J. J., Jiang, L. P., and Zhu, J. J., 2015. ACS applied materials & interfaces 7(4): 2979-2985.

Dong, Y., Dong, C., Wan, F., Yang, J., and Zhang, C., 2015. Science China Chemistry 58(10): 1515-1523.
Eckermann, A. L., Feld, D. J., Shaw, J. A., & Meade, T. J., 2010. Coordination chemistry reviews 254(15-16): 1769-1802.

Ertl, P., Emrich, C. A., Singhal, P., and Mathies, R. A., 2004. Analytical chemistry 76(13): 3749-3755.
Ezziane, Z., 2005. Nanotechnology 17(2): R27-39.

Flatt, A. K., Dirk, S. M., Henderson, J. C., Shen, D. E., Su, J., Reed, M. A., & Tour, J. M., 2003. Tetrahedron 59(43): 8555-8570.

Hanwell, M. D., Curtis, D. E., Lonie, D. C., Vandermeersch, T., Zurek, E., and Hutchison, G. R., 2012. Journal of cheminformatics 4(1): 17.

Hess, C. R., Juda, G. A., Dooley, D. M., Amii, R. N., Hill, M. G., Winkler, J. R., & Gray, H. B., 2003. Journal of the American Chemical Society 125(24): 7156-7157.

Hong, J., Zhao, Y. X., Xiao, B. L., Moosavi-Movahedi, A. A., Ghourchian, H., & Sheibani, N., 2013. Sensors 13(7): 8595-8611.

Laviron, E., 1979. Journal of Electroanalytical Chemistry and Interfacial Electrochemistry 101(1): 19-28.

Livshits, G. I., Stern, A., Rotem, D., Borovok, N., Eidelshtein, G., Migliore, A., Penzo, E., Wind, S. ., Di Felice, R., Skourtis, S. S., Cuevas, J. C., Gurevich, L., Kotlyar, A. B., and Porath, D., 2014. Nature nanotechnology 9(12): 1040-1046.

Love, J. C., Estroff, L. A., Kriebel, J. K., Nuzzo, R. G., and Whitesides, G. M., 2005. Chemical reviews 105(4): 1103-1170.

Lovgren, S., 2003. National Geographic News, 24.

Paleček, E., 1988. Analytical biochemistry 170(2): 421-431.

Porath, D., Bezryadin, A., De Vries, S., and Dekker, C., 2000. Nature 403(6770): 635.

Seiwert, B., and Karst, U., 2008. Analytical and bioanalytical chemistry 390(1): 181.

Shipman, S. L., Nivala, J., Macklis, J. D., and Church, G. M., 2017. Nature 547(7663): 345.

Swager, T. M., 1998. Accounts of Chemical Research 31(5): 201-207.

Trammell, S. A., Seferos, D. S., Moore, M., Lowy, D. A., Bazan, G. C., Kushmerick, J. G., and Lebedev, N., 2007. Langmuir 23(2): 942-948.

Ulgut, B., and Abruna., H. D., 2008. Chemical reviews 108(7): 2721-2736.

Umek, R. M., Lin, S. W., Vielmetter, J., Terbrueggen, R. H., Irvine, B., Yu, C. J., and Chen, Y. P., 2001. The Journal of Molecular Diagnostics 3(2): 74-84.

Xu, Y., Jiang, Y., Cai, H., He, P. G., and Fang, Y. Z., 2004. Analytica chimica acta 516(1-2): 19-27.

Yu, F., 2004. Max-Planck-Institute für Polymerforschung, Johannes Gutenberg-Universität, Mainz Doktor der Naturwissenschaft. Retrieved from http://www2.mpip-mainz.mpg.de/documents/akkn/publications/thesis/yu_2004.pdf

Zaffino, R. L., Mir, M., and Samitier, J., 2014. Nanotechnology 25(10): 105501-105509.

Highlights

- Study of S-[4-[2-[4-(2-Phenylethynyl)phenyl]ethynyl]phenyl] thiol as wiring molecule (MW)
- Co-immobilized SAM of MW and ss-DNA for hybridising with complementary ferrocene labelled.
- Key role played by the nanometric design of the capture probe linkers to achieve an efficient e- transport
- Electron transfer rate constant was calculated for the different platforms.
- The best MW/capture probe linker couple benefited on 8 times current signal